New Journal of Physics
The open access journal at the forefront of physics

Deutsche Physikalische Gesellschaft DPG
IOP Institute of Physics

Published in partnership with: Deutsche Physikalische Gesellschaft and the Institute of Physics

OPEN ACCESS

RECEIVED
12 August 2015

REVISED
23 December 2015

ACCEPTED FOR PUBLICATION
7 January 2016

PUBLISHED
5 February 2016

PAPER

Deterministic amplification of Schrödinger cat states in circuit quantum electrodynamics

Jaewoo Joo[1,2,5], **Matthew Elliott**[2], **Daniel K L Oi**[3], **Eran Ginossar**[2] **and Timothy P Spiller**[4]

[1] Quantum Information Science, School of Physics and Astronomy, University of Leeds, Leeds LS2 9JT, UK
[2] Advanced Technology Institute and Department of Physics, University of Surrey, Guildford, GU2 7XH, UK
[3] SUPA Department of Physics, University of Strathclyde, Glasgow, G4 0NG, UK
[4] York Centre for Quantum Technologies, Department of Physics, University of York, York YO10 5DD, UK
[5] Author to whom any correspondence should be addressed.

E-mail: j-w-joo@hanmail.net

Keywords: circuit quantum electrodynamics, cat states, amplification of quantum states, superconducting circuits, quantum optics

Abstract

Perfect deterministic amplification of arbitrary quantum states is prohibited by quantum mechanics, but determinism can be achieved by compromising between fidelity and amplification power. We propose a dynamical scheme for deterministically amplifying photonic Schrödinger cat states, which show great promise as a tool for quantum information processing. Our protocol is designed for strongly coupled circuit quantum electrodynamics and utilizes artificial atomic states and external microwave controls to engineer a set of optimal state transfers and achieve high fidelity amplification. We compare analytical results with full simulations of the open, driven Jaynes–Cummings model, using realistic device parameters for state of the art superconducting circuits. Amplification with a fidelity of 0.9 can be achieved for sizable cat states in the presence of cavity and atomic-level decoherence. This tool could be applied to practical continuous-variable information processing for the purification and stabilization of cat states in the presence of photon losses.

1. Introduction

Superpositions of two large coherent states with opposite phases, called Schrödinger cat states (SCSs) [1, 2], have great potential to open new avenues of research for quantum technology, including continuous-variable (CV) quantum communication [3], fault-tolerant quantum computation [4–6], CV teleportation [7], and quantum metrology [8, 9]. There is therefore particular interest in deterministic amplification schemes for these states, in order to protect them from photon loss in addition to studying fundamental aspects of amplification. If moderate sized SCSs—large enough that the coherent states have little overlap, but small enough to prevent excessive decoherence by photon loss—can be produced and stabilized, then fault-tolerant CV quantum computing is possible using only linear optics. It is known that two identical SCSs can deterministically produce a larger SCS [10, 11], while several high-fidelity probabilistic methods of amplifying SCSs have recently been developed in quantum optics [7, 12].

Quantum physics does not allow perfect deterministic amplification of unknown quantum states because additional quantum noise is inevitably introduced by the amplification process [13]. The most commonly studied methods of high fidelity amplification of coherent states (i.e. $|\alpha\rangle \rightarrow |G\alpha\rangle$ for $G > 1$) are based on probabilistic addition and subtraction of single photons [14]. The fidelity and amplification factor G of these processes vary differently with input amplitude α, depending on the amplification operator that is implemented [15–17]. For example, the probabilistic amplification operators $\hat{a}\hat{a}^{\dagger}$ and $(\hat{a}^{\dagger})^2$ have recently been investigated [17]. Such schemes are always restricted by the tradeoff between amplification factor and fidelity, as perfect amplification is forbidden by the no-cloning theorem [15].

The recent rapid development of superconducting circuit technology has provided a possible new platform for scalable quantum systems. The Josephson junction nonlinearity allows the realization of superconducting

artificial atoms (qubits) which can be strongly coupled to 3D cavities containing nonclassical microwave states. Sufficiently large SCSs for applications in quantum information ($\alpha \approx 2$) [18, 19] and generalized Fock states [20] have recently been generated in microwave cavities with the assistance of superconducting qubits. Moreover, enhanced stabilization of SCSs in a cavity has recently been reported using a specially designed lossy environment [18, 21], with the aim of producing robust quantum memory [22]. This loss engineering could also provide a complementary (continuous) method of SCS amplification in circuit QED. Further progress in using these states for information processing, however, requires that we understand the limits of control in a large state space (in principle infinite-dimensional for a CV cavity state) and the use of pulse control techniques in experimental setups has so far been limited. Amplification of SCSs would benefit a wide range of hybrid-state quantum technologies, and enable a new type of quantum computation within the framework of circuit-quantum electrodynamics (circuit QED) [23].

In this paper, we propose a scheme for amplifying an SCS in superconducting circuits. The key benefit of this atom-assisted method is that it is deterministic while other amplification schemes in optics are highly probabilistic. Heralded optics methods add and remove photons through a beamsplitter and successful amplification of the input state occurs conditionally on detection of the photons. In our scheme, atomic excited states can repeatedly be prepared by controlled microwave pulses and the core of the amplification operation is performed as a unitary generalized σ_x operation on the dressed atomic-photonic states. Consequently, it does not require any specific loss engineering to achieve stabilisztion of the state. Our scheme is based on the observation that applying the bare two-photon shift operation [2], $(\hat{E}^\dagger)^2 : |m\rangle \longrightarrow |m+2\rangle \forall\, m$, one or more times to an even/odd SCS shifts the number state distribution while preserving their relative amplitudes. We achieve this by using a set of overlapping microwave pulses to climb the Jaynes–Cummings (JC) ladder. This technique is also applicable to other protocols where precise state transfers are required. We analyse and simulate the operation $\hat{E}^\dagger$ and $(\hat{E}^\dagger)^2$ acting on an even SCS ($\alpha = 1.5$) in a cavity–qubit system in the presence of decoherence [24], finding microwave pulse controls which perform all the state-transfers required with high fidelity and within the decoherence time of realistic circuit QED systems based on transmons and high-Q cavities.

2. Theoretical $(\hat{E}^\dagger)^2$ amplification of SCSs

We generalize the notion of amplification to the case where an initial even/odd SCS

$$|\mathrm{SC}_\alpha^\pm\rangle = \mathcal{N}_\alpha^\pm(|\alpha\rangle \pm |-\alpha\rangle), \tag{1}$$

with some normalization $\mathcal{N}_\alpha^\pm$, is transformed by an operation $\hat{A}$ into a state $\hat{A}|SC_\alpha^\pm\rangle$, which approximates a larger SCS

$$|\mathrm{SC}_{\alpha'}^\pm\rangle \approx \hat{A}|SC_\alpha^\pm\rangle = \sum_{k=0}^{\infty} c_k |k+b\rangle\langle k|\mathrm{SC}_\alpha^\pm\rangle, \tag{2}$$

with $\alpha' > \alpha$ and $b > 0$. Due to destructive interference between $|\alpha\rangle$ and $|-\alpha\rangle$, even SCSs have only even photon numbers while odd SCSs have only odd photon numbers. The amplitudes c_k are determined by the amplification operator $\hat{A}$.

If we choose the amplification operator to be the two-photon shift operator applied l times

$$\hat{A} = (\hat{E}^\dagger)^{2l} = \sum_{m=0}^{\infty} |m+2l\rangle\langle m|, \tag{3}$$

the Fock state amplitude distribution is simply shifted and the normalization of the outcome state is preserved. It can therefore be performed deterministically in principle [25]. Figure 1 shows the results of applying $(\hat{E}^\dagger)^2$ to both even and odd SCSs and calculating the overlap of an amplified SCS $(\hat{E}^\dagger)^2|\mathrm{SC}_\alpha^\pm\rangle$ with a target SCS $|\mathrm{SC}_{\alpha'}^\pm\rangle$, where the fidelities are calculated as

$$\mathcal{F}^\pm = |\langle \mathrm{SC}_{\alpha'}^\pm|(\hat{E}^\dagger)^2|\mathrm{SC}_\alpha^\pm\rangle|^2. \tag{4}$$

We quantify the amplification by the value G, defined by $\alpha' = G\alpha$ which maximizes $\mathcal{F}^\pm$, giving the closest SCS to $(\hat{E}^\dagger)^2|\mathrm{SC}_\alpha^\pm\rangle$

$$G = \arg\max_{G'} |\langle \mathrm{SC}_{G'\alpha}^\pm|(\hat{E}^\dagger)^2|\mathrm{SC}_\alpha^\pm\rangle|^2. \tag{5}$$

In general, the maximum fidelity $\mathcal{F}_{\max}^\pm$ approaches 1 for large α but G also tends to 1, indicating minimal amplification of very large SCSs, but stabilization of the input SCS persists. We show fidelities between $(\hat{E}^\dagger)^2|\mathrm{SC}_\alpha^\pm\rangle$ and ideal amplified state $|\mathrm{SC}_{G\alpha}^\pm\rangle$ for $\alpha = 1.0,\ 1.5,\ 2.0,\ 2.5$. The $\mathcal{F}_{\max}^+$ are 0.854, 0.947, 0.974, 0.988, corresponding to $G \approx 1.725,\ 1.377,\ 1.229,\ 1.151$, while the $\mathcal{F}_{\max}^-$ are 0.681, 0.866, 0.960, 0.987

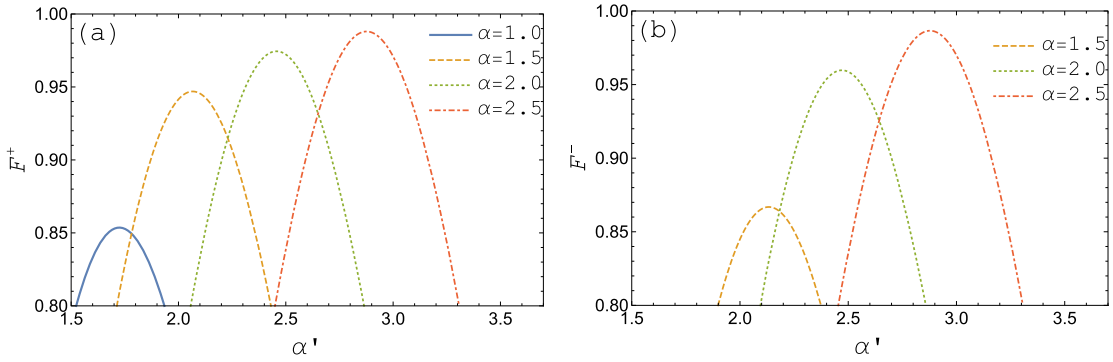

Figure 1. Fidelities $\mathcal{F}^{\pm}$ between $(\hat{E}^{\dagger})^2|\mathrm{SC}_{\alpha}^{\pm}\rangle$ and amplified state $|\mathrm{SC}_{\alpha'}^{\pm}\rangle$ for $\alpha = 1.0, 1.5, 2.0, 2.5$. The maximum fidelities approach 1 for large α while the amplification rate defined in equation (5) also goes to unity, demonstrating the fundamental tradeoff between the fidelity and amplification rate. For small α, $(\hat{E}^{\dagger})^2$ works better for even SCSs, but this difference between even and odd SCSs disappears for $\alpha > 1.5$ as $|\alpha\rangle$ and $|-\alpha\rangle$ become non-overlapping.

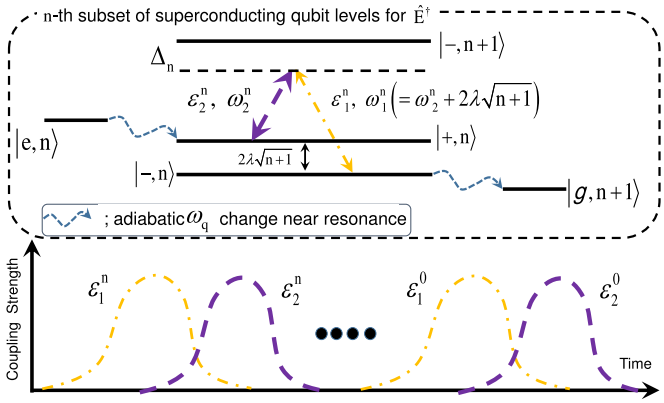

Figure 2. STIRAP-type pulse sequence to realize $\hat{E}^{\dagger}$ for nth number state $|n\rangle$. (Top) An adiabatic sweep of the qubit frequency ω_q into resonance with the cavity ω_r transforms the initial state $|e, n\rangle$ into the dressed state $|+, n\rangle$. Next a microwave field is applied to the $|-, n\rangle \leftrightarrow |-, n+1\rangle$ transition with time dependent Gaussian amplitude $\epsilon_1^n(t)$ and frequency ω_1^n (yellow dotted–dashed line), followed by another field driving the second transition ($|+, n\rangle \leftrightarrow |-, n+1\rangle$) with envelope $\epsilon_2^n(t)$ and frequency ω_2^n (purple dashed line). For an SCS, the $|-, n+1\rangle$ state is unpopulated hence does not participate in the dynamics. The microwave frequencies are detuned by Δ_n from the $|-, n+1\rangle$ state but satisfy the two-photon transition condition, $\omega_1^n - \omega_2^n = 2\lambda\sqrt{n+1}$. After the pulse sequence, a further adiabatic sweep of the transmon frequency back out of resonance disentangles the atom from the cavity, resulting in the state $|g, n+1\rangle$. The action on the cavity state is $|n\rangle \rightarrow \hat{E}^{\dagger}|n\rangle = |n+1\rangle$. (Bottom) If the input state is an even SCS given by $\sum c_n|n\rangle$, a set of pulses $\{\epsilon_1^n(t), \epsilon_2^n(t)\}$ acting on each number state produces the outcome state $\sum c_n|n+1\rangle$.

with $G \approx 1.902, 1.422, 1.235, 1.151$. Interestingly, for $\alpha < 1.5$, $(\hat{E}^{\dagger})^2$ works better for even SCSs because $|\mathrm{SC}_{\alpha\approx 0}^{-}\rangle$ is approximately a one-photon-Fock state. When shifted, this a mapped to a three-photon Fock state, which is very different to any odd SCS and we find that $\mathcal{F}_{\max}^{-} < 0.8$ for $\alpha = 1.0$. This behavior disappears for $\alpha \geqslant 1.5$ because $|\alpha\rangle$ is sufficiently orthogonal to $|-\alpha\rangle$. Thus, we will focus on how to implement the amplification procedure for an SCS with $\alpha = 1.5$, in the range of interest for CV quantum information processing.

3. Implementation in circuit QED

Circuit QED provides an ideal regime for amplification of SCSs, due to the large nonlinearities and strong couplings that can be achieved. We first outline our scheme for performing a single $\hat{E}^{\dagger}$ operation on a cavity field, with further details of the implementation in the following sections. This operation can be applied twice to achieve $(\hat{E}^{\dagger})^2$, and therefore amplification of SCSs. The protocol, shown in figure 2, is as follows: (1) an SCS $|\mathrm{SC}_{\alpha}^{\pm}\rangle = \sum_{n=0}^{\infty} c_n|n\rangle$ is initially prepared in the cavity, where the c_n vanish for odd (even) n for even (odd) SCSs, with the qubit in $|e\rangle$. (2) An adiabatic sweep is used to bring the qubit frequency ω_q from far off-resonance to the resonator frequency ω_r, where the eigenstates of the system are dressed qubit-cavity states [24]. This slowly transfers the bare system into a superposition of dressed states $\sum_{n=0}^{\infty} c_n|+, n\rangle$. (3) A state-transfer scheme

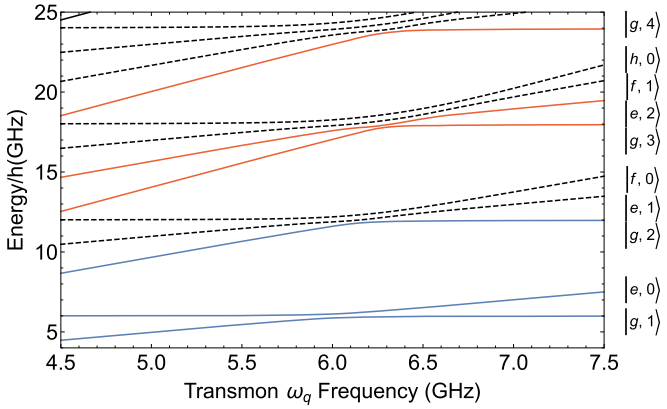

Figure 3. Energy level structure of a transmon coupled to a cavity with $\omega_r/2\pi = 6$ GHz and $\lambda/2\pi = 0.1$ GHz [30]. Solid lines indicate two sets of Λ-type dressed levels $\{|+, n\rangle, |-, n\rangle, |-, n+1\rangle\}$ suitable for state-transfers and dashed lines are other eigenstates of the Hamiltonian in equation (6) [24, 33]. The labels on the right-hand side are the product states that approximate the eigenstates for large positive detunings ($\omega_q - \omega_r \gg \lambda$).

adapted from the original idea of stimulated Raman adiabatic passage (STIRAP) in cavity-QED [26–29] is performed. Instead of using a bare atomic Λ-level configuration, we use a set of Λ-type systems in the dressed JC model, with dynamical control provided by varying local fluxes [30, 31]. Pairs of overlapping Gaussian microwave pulses are applied to the effective three-level systems $\{|+, n\rangle, |-, n\rangle, |-, n+1\rangle\}$ to transfer the populations into the state $\sum_{n=0}^{\infty} c_n|-, n\rangle$, via the $|-, n+1\rangle$ states. (4) The first step is reversed, sweeping ω_q away from ω_r to disentangle the final cavity state from the qubit, leaving it in the state $\sum_{n=0}^{\infty} c_n|n+1\rangle \approx |\mathrm{SC}_{\alpha'}^{\mp}\rangle$ which has $\alpha' > \alpha$ and opposite parity.

To repeat the operation, the qubit must be reset from $|g\rangle$ to $|e\rangle$ by a further microwave pulse, but it is now sufficiently far detuned that the cavity state is not significantly affected. Finally, after the second $\hat{E}^{\dagger}$ operation, we apply a selective number-dependent arbitrary phase (SNAP) gate to correct relative phases between Fock states that are acquired during the operation. This technique has been already demonstrated in a protocol to minimize phase distortions due to self-Kerr interactions [32].

3.1. Adiabatic sweep of qubit frequency ω_q

We model a transmon qubit coupled to a cavity by a generalized JC Hamiltonian

$$\hat{H}^t = \omega_r \hat{a}^{\dagger}\hat{a} + \sum_j \frac{\omega_{qj}}{2}|j\rangle\langle j| + \sum_{j,k}\lambda_{j,k}(\hat{a}^{\dagger}|j\rangle\langle k| + \hat{a}|k\rangle\langle j|), \tag{6}$$

for transmon energy levels $j, k = \{g, e, f, h, \ldots\}$ and transmon-cavity couplings $\lambda_{j,k}$. As shown in figure 3, when the transmon frequencies are far from resonance with the cavity, the bare states are given by $|j, n\rangle$ with transmon state j and photon number n, while they become dressed states near resonance. We now approximate the transmon as a two-level system as, in practice, the additional levels of the transmon do not negatively affect the protocol. We discuss the impact of including a third transmon level in appendix B. Considering only two transmon levels, $\{|g\rangle, |e\rangle\}$, the eigenstates are

$$|+, n\rangle = \cos\theta_n|e, n\rangle + \sin\theta_n|g, n+1\rangle, \tag{7}$$

$$|-, n\rangle = -\sin\theta_n|e, n\rangle + \cos\theta_n|g, n+1\rangle, \tag{8}$$

where $\omega_q = \omega_{qe} - \omega_{qg}$ is the qubit transition frequency, $\lambda = \lambda_{g,e}$ is the qubit–cavity coupling, and $2\theta_n = \tan^{-1}(2\lambda\sqrt{n+1}/\delta)$, with $\delta = \omega_q - \omega_r$. Note that $|+, n\rangle \approx |e, n\rangle$ and $|-, n\rangle \approx |g, n+1\rangle$ for large δ, so if we start in $|e, n\rangle$ far from resonance, the state adiabatically becomes $|+, n\rangle$ as ω_r approaches resonance $\delta \approx 0$. This process requires the use of flux-tunable qubits. In realistic devices with multiple transmon levels, this sweeping must be performed slowly enough to prevent leakage of population to higher levels.

3.2. Protocol for state-transfer on even SCSs in circuit-QED

The key element of our $\hat{E}^{\dagger}$ operation is an efficient state transfer from $|+, n\rangle$ to $|-, n\rangle$ which is performed on individual number states using Λ-type sets of levels. Once the initial, dressed state is prepared a microwave field is first applied between $|-, n\rangle$ and $|-, n+1\rangle$ with time dependent amplitude $\epsilon_1^n(t) = |\epsilon_1^n|\exp[-(t-\tau)^2/T^2]$ and frequency ω_1^n, followed by another field driving the $|+, n\rangle \leftrightarrow |-, n+1\rangle$ transition ($\epsilon_2^n(t) = |\epsilon_2^n|\exp[-(t+\tau)^2/T^2]$, ω_2^n). Both drives are detuned by Δ_n from

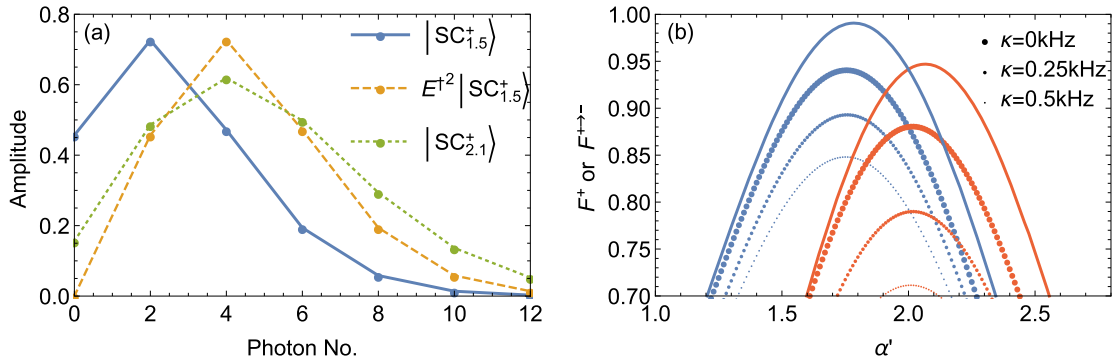

Figure 4. (a) Photon number amplitudes for states $|SC^{+}_{1.5}\rangle$, $(\hat{E}^{\dagger})^2|SC^{+}_{1.5}\rangle$ and $|SC^{+}_{2.1}\rangle$. We see that the population of the eight-photon-Fock state is less than 1% for $|SC^{+}_{1.5}\rangle$ and that therefore four sets of state-transfers cover enough levels for amplifying these states. (b) Fidelities $\mathcal{F}^{+\to -}$ (blue) and $\mathcal{F}^{+}$ (red) achieved by applying $\hat{E}^{\dagger}$ and $(\hat{E}^{\dagger})^2$ respectively to $|SC^{+}_{1.5}\rangle$. The solid lines show the theoretical bounds, which are $\mathcal{F}^{+\to -}_{\max} > 0.99$ at $\alpha' \approx 1.78$ and $\mathcal{F}^{+}_{\max} > 0.945$ at $\alpha' \approx 2.1$. The dotted lines show the simulated performance with different values of decoherence ($\gamma_{-} = \gamma_{\phi} = 10\kappa$) using four sets of simultaneous state-transfer operations. An amplification factor of $G \approx 1.33$ is achieved for $(\hat{E}^{\dagger})^2$.

their respective transitions, while still satisfying the two photon condition $\omega_1^n - \omega_2^n = 2\lambda\sqrt{n+1}$, which ensures that the intermediary $|-, n+1\rangle$ state is not populated. The pulses have a region of overlap, determined by the temporal offset τ. For efficient transfer of $|+, n\rangle \to |-, n+1\rangle$, we require $\tau > (\sqrt{2} - 1)T$ and $|\epsilon|T \gg 10$ [34].

A pair of pulses is used to transfer each number state with significant population. For an even SCS, all odd-number states are unpopulated, so the Λ systems are effectively independent of each other. This spacing of occupied and unoccupied states also prevents spectral crowding and the driving of unwanted transitions. The pulses are performed in the manifolds of dressed states $\{|+, n\rangle, |-, n\rangle, |-, n+1\rangle\}$, in order, from the nth to 0th manifold. After all pulse sets and disentanglement from the qubit, this leaves the final state $\sum c_n|n+1\rangle = \hat{E}^{\dagger}\sum c_n|n\rangle$. We see that $\hat{E}^{\dagger}$ flips the even SCSs to odd. Note that the analytical (theoretical) fidelity between $|SC^{-}_{\alpha'}\rangle$ and $\hat{E}^{\dagger}|SC^{+}_{\alpha}\rangle$ is given by

$$\mathcal{F}^{+\to -} = |\langle SC^{-}_{\alpha'}|\hat{E}^{\dagger}|SC^{+}_{\alpha}\rangle|^2. \tag{9}$$

Figure 4(b) shows that the maximum theoretical fidelity $\mathcal{F}^{+\to -}_{\max}$ is higher than 0.99 between $\hat{E}^{\dagger}|SC^{+}_{1.5}\rangle$ and $|SC^{-}_{1.78}\rangle$.

The scheme discussed here is compatible with the existing protocol for creating SCSs in [19], while conventional STIRAP and two-tone red sideband transitions have also been demonstrated in Λ-type superconducting systems [34–36].

3.3. Protocol for $(\hat{E}^{\dagger})^2$ and SNAP gates

In contrast to cavity QED STIRAP setups, where atoms are passed through the cavity [27], π-pulses can be used to reset the qubit state $|g\rangle \to |e\rangle$ directly without affecting the cavity state [19], and hence $(\hat{E}^{\dagger})^2$ can, in principle, be performed by repeating the protocol. The overall fidelity is reduced by Kerr-type nonlinearities in the dressed cavity, causing defects which accumulate over time. However, these distortions can be significantly reduced by using a SNAP gate [32] to compensate for the relative phases acquired by different number states. These gates have been experimentally demonstrated in a dispersively coupled superconducting cavity-qubit system. The dispersive energy shifts of the cavity due to the qubit allow individual Fock states to be addressed by microwaves drives of appropriate frequencies. Thus, n microwaves can perform a sum of phase gates on Fock states $|m\rangle$ given by $S_{\text{snap}} = \sum_{m=0}^{n-1} \exp(i\Phi_m)|m\rangle\langle m|$. As the procedure is limited by the decoherence time and these distortions, we examine both $\hat{E}^{\dagger}$ and $(\hat{E}^{\dagger})^2$ including qubit and cavity decoherence, along with corrections by SNAP gates.

4. Simulation with decoherence

To examine the performance of the protocol, we numerically simulate a simplified driven JC Hamiltonian with two atomic levels [37–39]

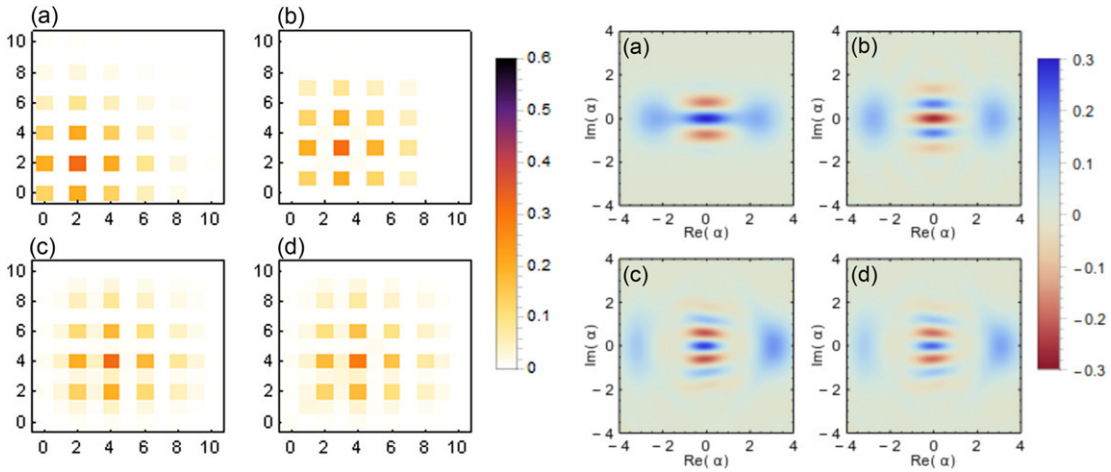

Figure 5. Density matrix amplitude plots c_{nm} (left) and Wigner functions (right). The initial state $|\mathrm{SC}^{+}_{1.5}\rangle$ is plotted in (a), with numerical $\hat{E}^{\dagger}|\mathrm{SC}^{+}_{1.5}\rangle \approx |\mathrm{SC}^{-}_{1.8}\rangle$ without decoherence shown in (b). Simulated two-photon shift with $(\hat{E}^{\dagger})^2$ is shown in (c) and, finally, (d) shows the final state $(\hat{E}^{\dagger})^2|\mathrm{SC}^{+}_{1.5}\rangle \approx |\mathrm{SC}^{+}_{2.1}\rangle$ including decoherence of $\kappa/2\pi = 0.25$ kHz. In the density matrix plots, the shifted blocks clearly indicate the $\hat{E}^{\dagger}$ and $(\hat{E}^{\dagger})^2$ are performed, with blurred regions caused by imperfect state-transfers and decoherence. In the Wigner function plots, interference fringes can be clearly seen, with the central fringe changing color between even and odd SCSs, while some distortions are caused by imperfect transfers. Decoherence slightly reduces the color contrast of fringe patterns between (c) and (d).

$$\hat{H}^{\mathrm{tot}} = \omega_{\mathrm{r}}\left(\hat{a}^{\dagger}\hat{a} + \frac{1}{2}\right) + \frac{\omega_{\mathrm{q}}}{2}\hat{\sigma}^{z} + \lambda(\hat{a}^{\dagger}\hat{\sigma}^{-} + \hat{a}\hat{\sigma}^{+}) + \sum_{n}\sum_{j=1}^{2}\epsilon_{j}^{n}(t)(\mathrm{e}^{-\mathrm{i}\omega_{j}^{n}t}\,\hat{a} + \mathrm{e}^{\mathrm{i}\omega_{j}^{n}t}\,\hat{a}^{\dagger}), \tag{10}$$

where ω_j^n are the frequencies of the microwave drives, and ϵ_j^n their amplitudes. While the microwave driving terms couple all of the excitation subspaces of the undriven JC Hamiltonian, the Hamiltonian is only slightly perturbed for small $|\epsilon_j|$ and the pulse frequencies are far off-resonance from unwanted transitions. Thus, the majority of the evolution is confined to the respective $\{|\pm, n\rangle\}$ manifold. The bichromatic driving induces the transition $|+, n\rangle \rightarrow |-, n\rangle$ via quasi-adiabatic following even though the system is not at, or close to, an eigenstate of the instantaneous Hamiltonian for part of the pulse sequence. This exploits the topological properties of the dressed eigenenergy surfaces [40]. We briefly note that this procedure in the driven JC system has a different character to conventional STIRAP on a bare Λ-level atom with directly driven transitions and behaves reversibly due to the unitary nature of the evolution (see figure A1 in appendix A).

4.1. $\hat{E}^{\dagger}$ and $(\hat{E}^{\dagger})^2$ with SNAP gates on $|\mathrm{SC}^{+}_{1.5}\rangle$

We first simulate a single $\hat{E}^{\dagger}$ operation acting on $|\mathrm{SC}^{+}_{1.5}\rangle$. In order to perform $\hat{E}^{\dagger}$ efficiently and practically, the minimum number of STIRAP-type sets can be decided by the plotting the number distribution of SCSs. Figure 4(a) shows that $|\mathrm{SC}^{+}_{1.5}\rangle$ has almost all of its population in four Fock states, $\{|0\rangle, |2\rangle, |4\rangle, |6\rangle\}$, and therefore four sets of STIRAP-type pulses will cover enough population to achieve good amplification. To minimize the length of the procedure and hence to reduce decoherence to practical levels, we perform all the transfers simultaneously, sharing a common first pulse. This produces almost identical fidelities to four independent state-transfer sets in the decoherence-free case, with large improvements when decoherence is included.

Our simulated system has $\lambda/2\pi = 0.1$ GHz and $\omega_{\mathrm{r}}/2\pi = 6.0$ GHz. We start with the qubit 1 GHz detuned and perform the adiabatic sweep in 6.2 μs, which is sufficiently slow to prevent population transfer to unwanted levels. For the four sets of state transfers, we use a single ω_1 which is shared between all transfers, adjusting Δ_i for each Λ-level system to find the appropriate value of ω_2^i. For the the first $\hat{E}^{\dagger}$ we use $\tau = 3.58$ μs and $T = 6.28$ μs, with other parameters given in table C1. With these parameters, the total state-transfer time is approximately 35 μs, which could be reduced further by using a larger transmon–cavity coupling strength. For the second $\hat{E}^{\dagger}$, $\tau = 3.14$ μs and $T = 6.28$ μs. In the Fock basis, SNAP gates are given by S_{snap}. The values of the phases are dependent on Fock states $|m\rangle$ and we choose $\{\Phi_m | m = 0, 1, \ldots, 8\}$ as given in appendix B.

To model Markovian decoherence associated with cavity and qubit decoherence, we use a Lindblad master equation

$$\dot{\rho} = \mathrm{i}[\hat{H}^{\mathrm{tot}}, \rho] + \kappa\mathcal{D}[\hat{a}] + \gamma_{-}\mathcal{D}[\hat{\sigma}^{-}] + \frac{\gamma_{\phi}}{2}\mathcal{D}[\hat{\sigma}^{z}], \tag{11}$$

where $\mathcal{D}[\hat{b}] = \hat{b}\rho\hat{b}^\dagger - \frac{1}{2}\{\hat{b}^\dagger\hat{b}, \rho\}$. We choose $\gamma_-/2\pi = \gamma_\phi/2\pi = 10\kappa/2\pi = 2.5,\ 5.0$ kHz using realistic parameters from [41]. The results are shown in figures 4 and 5. In figure 4(a), a comparison of the photon number amplitudes for $|\mathrm{SC}^+_{1.5}\rangle$, $(\hat{E}^\dagger)^2|\mathrm{SCS}^+_{1.5}\rangle$ and $|\mathrm{SC}^+_{2.1}\rangle$ indicates the similarity of the amplified SCS and the desired target SCS. As shown in figure 4(b), $\hat{E}^\dagger$ without decoherence achieves a maximum fidelity above 0.94, with the gap between the theoretical and no-decoherence cases caused by imperfections in the transfer method and partly due to a small population of higher dressed states over $|+, 8\rangle$, which are not transferred. The dotted points show that decoherence almost linearly reduces the fidelity, with $\mathcal{F}^{+\to-} \approx 0.9$ and $\mathcal{F}^+ \approx 0.8$ for $\kappa/2\pi = 0.25$ kHz.

4.2. Evidence of performing $(\hat{E}^\dagger)^k$ on $|\mathrm{SC}^+_{1.5}\rangle$ ($k = 1, 2$)

It is straightforward to show the performance of the shift operation $(\hat{E}^\dagger)^k$ by looking at the density matrices of the initial and final states, because the components of the density matrix of SCSs are shifted by k Fock-basis elements. For example, the density matrix of an initial even SCS is

$$\rho_{\mathrm{int}} = |\mathrm{SC}^+_\alpha\rangle\langle\mathrm{SC}^+_\alpha| = \sum_{n,m=0}^{\infty} c_{nm}|2n\rangle\langle 2m|. \tag{12}$$

After the shift operation has been performed, the outcome state is given by

$$\rho_{\mathrm{out}} = (\hat{E}^\dagger)^k|\mathrm{SC}^+_\alpha\rangle\langle\mathrm{SC}^+_\alpha|(\hat{E})^k = \sum_{n,m=0}^{\infty} c_{nm}|2n+k\rangle\langle 2m+k|. \tag{13}$$

Plots of magnitude of density matrix elements (left side) and Wigner plots of the states (right side) are shown in figure 5. Panels marked (a) show the initial SCS, which one can assume is prepared using the method of [19]. In (b) the state after applying a single $\hat{E}^\dagger$ followed by SNAP gates is shown. In (c), the $(\hat{E}^\dagger)^2$ operation is performed with a qubit flip after the first $\hat{E}^\dagger$ and the SNAP gates after the second $\hat{E}^\dagger$. Finally (d) includes decoherence with $\kappa/2\pi = 0.25$ kHz.

We see that without decoherence the coefficients c_{nm} are preserved but shifted. With decoherence, there is blurring of this effect as odd number states become populated. This type of quantum process tomography can be performed experimentally. In the Wigner functions, the interference fringes clearly switch between negative and positive values as the SCS switches between odd and even parity, with a central blue peak in (a), (c) and (d) while in (b) the central peak is red. In (d), we see that the decoherence slightly reduces the contrast of the fringe patterns but the state is clearly very similar to the no-decoherence case shown in (c). Using Ramsey interferometry, one can measure the qubit state-dependent phase shift of the cavity state, as explained in the supplementary material of [19], and therefore perform tomography on the state in the high-Q cavity via a low-Q cavity. Alternatively, a parity measurement can also be used to show the parity difference between the initial and final states [42].

Overall, the total operation time for our $(\hat{E}^\dagger)^2$ protocol is approximately 96 μs, including four adiabatic sweeps to bring in and out the qubit (24.8 μs), two applications of the STIRAP-type operations (70 μs), a qubit-flip to reset the qubit, and SNAP gates (1 μs). Very recently, the experimental group at Yale University has developed a superconducting cavity qubit system with a single photon decay lifetime of 1.22 ms [43]. Including all aspects of the total time, this would allow us to perform roughly 12 repetitions of our $(\hat{E}^\dagger)^2$ protocol before a photon is lost. This is achieved without the use of any optimization techniques, which we expect would reduce the operation time further. Additionally, cat state preparation (0.5 μs) and a parity measurement (0.4 μs) for Wigner tomography are required to verify the protocol, but do not contribute significantly to the time of the protocol (see experimental papers in [19]).

5. Summary and remarks

We have demonstrated a scheme for deterministic amplification of microwave SCSs using $\hat{E}^\dagger$ and $(\hat{E}^\dagger)^2$ operations in circuit QED. A STIRAP-type state transfer method provides the core of the $\hat{E}^\dagger$ operation, which simply shifts the Fock state amplitude distribution of the initial SCS. The theoretical scheme is compared with the simulation of the JC model with three values of decoherence. The application of $\hat{E}^\dagger$ amplifies an even SCS $|\mathrm{SC}^+_{1.5}\rangle$ to an odd SCS $|\mathrm{SC}^-_{\approx 1.8}\rangle$ with the fidelity 0.9 under realistic decoherence, while $(\hat{E}^\dagger)^2$ produces $|\mathrm{SC}^+_{\approx 2.0}\rangle$ with fidelity 0.8. Due to the benefits of the superconducting system, this deterministic method overcomes the problems associated with probabilistic optics-only amplification methods, useful for other applications in the future. Dissipation engineering solutions provide a complementary scheme for continuously amplifying SCSs [18], while our discretized scheme could be extended to amplification of bipartite (or multipartite) entangled SCSs without specially designed lossy environments [8, 9, 44]. We note that a related experiment has been recently performed with coherent states in an ion-trap system and this could use shortcuts to adiabaticity to reduce the time required (e.g., using counter-diabatic controls) [45].

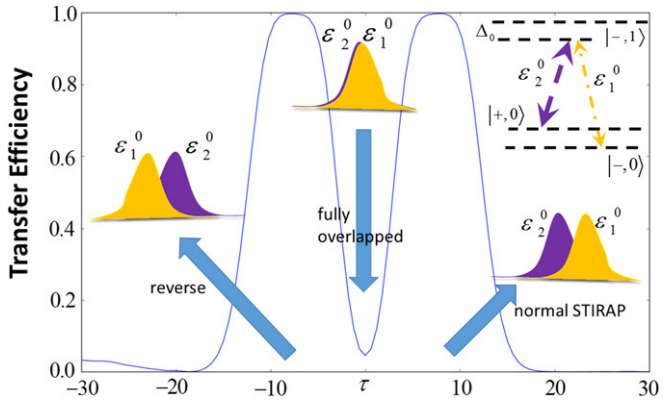

Figure A1. Transfer efficiency of the STIRAP-type pulses between $|+,0\rangle$ and $|-,0\rangle$ as a function of the overlap between the two pulses. This provides evidence that our state-transfer scheme is a generalized σ_x operation between $|+,n\rangle$ and $|-,n\rangle$ for different n.

In CV quantum information processing using SCSs, $\hat{E}^\dagger$ can be used as a bit-flip operation, by switching the state parity with minimal amplification for $\alpha > 2$, while $(\hat{E}^\dagger)^2$ can act as a stabilizer operation on SCSs. If one can perform either $\hat{E}^\dagger$ or $(\hat{E}^\dagger)^2$ depending on the outcome of a parity measurement of the cavity state, it can be used for a discretized purification of SCSs. Taking advantage of well-separated lower energy levels, fluxonium or flux qubits could also be used in this scheme [46].

Acknowledgments

We would like to thank J Dunningham for early contributions to this project and H Jeong and B Vlastakis for useful comments. EG and TPS acknowledge support from EPSRC (EP/L026082/1 and EP/M013472/1, respectively). DKLO acknowledges the Quantum Information Scotland (QUISCO) network. The data underlying this work is available without restriction (doi: 10.15126/surreydata.00709736).

Appendix A. Evidence of STIRAP-type operations

Although this STIRAP-type operation behaves well enough for our desired state-transfer ($|+,n\rangle \rightarrow |-,n\rangle$), it cannot be fully explained by conventional STIRAP in a bare Λ atomic system. In STIRAP, the state tranfer efficiency is strongly dependent on the overlap of the two pulse envelopes [47]. In particular, efficient state-transfer only occurs for the counter-intuitive sequence of the two pulses (ϵ_1 first and ϵ_2 second).

We have examined the transfer efficiency of our scheme for the simplest transfer from $|+,0\rangle$ to $|-,0\rangle$ with detuning Δ_0 in figure A1. For positive τ, the behavior is similar to the normal STIRAP counter-intuitive pulse sequence, with transfer efficiency rapidly approaching 1 as τ increases. The efficiency then drops with decreasing overlap area. However, our operation also shows excellent state-transfer for the reverse pulse sequence. It therefore behaves like a generalization of the σ_x operation on the cavity state.

In our parameter region, and without decoherence, the transfer efficiency is symmetric about $\tau = 0$ (fully overlapped pulses). However, the transfer efficiency for reversed pulses is more sensitive to changes in Δ_0 and the length of pulse envelopes. Oscillations are seen in the transfer efficiency, indicating that the process may not be 'as adiabatic' as conventional STIRAP. These phenomena might be better understood in adiabatic Floquet theory [48] and we believe they are caused by the existence of energy levels outside the Λ-system [49].

Appendix B. Additional transmon levels

As the transmon is in fact a multilevel system, there is the potential for additional levels to affect the state transfer. We therefore simulated a single STIRAP-type state transfer from the $|0,+\rangle$ state to the $|0,-\rangle$ state both with and without a third transmon level. The results are shown in figure B1. While the frequencies of the microwave must be adjusted to fit the new energy levels of the system, the pulse envelopes, their amplitudes and overlaps are identical. Crucially this means that the transfer does not have to be performed more slowly when a realistic transmon is introduced.

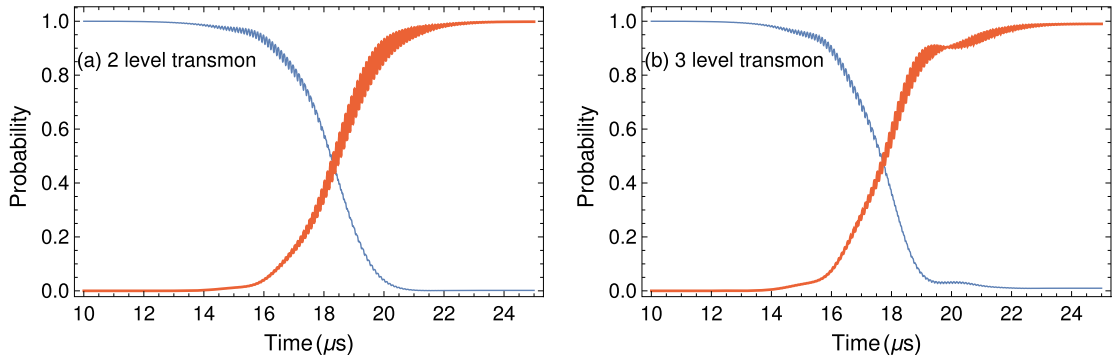

Figure B1. Comparison of the population transfer via the STIRAP-type pulses from $|+,0\rangle$ (blue) to $|-,0\rangle$ (red) in (a) two levels and (b) three levels of the transmon. This indicates that while the third transmon level affects the transfer process, it does not affect the final fidelity.

Appendix C. Simulation parameters for SNAP gates and state-transfers

Table C1. Simulation parameters used for the first $\hat{E}^{\dagger}$ (top half) and second $\hat{E}^{\dagger}$ (bottom half).

Transfer	$\epsilon_1/2\pi$ (MHz)	$\omega_1/2\pi$ (GHz)	$\epsilon_2/2\pi$ (MHz)	$\omega_2/2\pi$ (GHz)	$\Delta/2\pi$ (MHz)
$\|0\rangle \rightarrow \|1\rangle$	10	5.949	35	5.749	10
$\|2\rangle \rightarrow \|3\rangle$	10	5.949	38	5.603	24
$\|4\rangle \rightarrow \|5\rangle$	10	5.949	49	5.501	30
$\|6\rangle \rightarrow \|7\rangle$	10	5.949	70	5.419	33
$\|1\rangle \rightarrow \|2\rangle$	24	5.953	55	5.679	15
$\|3\rangle \rightarrow \|4\rangle$	24	5.953	36	5.551	22
$\|5\rangle \rightarrow \|6\rangle$	24	5.953	32	5.462	26
$\|7\rangle \rightarrow \|8\rangle$	24	5.953	31	5.385	29

Table C2. Values of phases used for different Fock states $|m\rangle$ for SNAP gates.

m	0	1	2	3	4	5	6	7	8
Φ_m	0	−1.589	−0.716	−0.907	3.037	−1.621	2.009	2.859	−0.573

References

[1] Schrödinger E 1935 *Naturwissenschaften* **23** 823
[2] Gerry C C and Knight P L 2005 *Introductory Quantum Optics* (Cambridge: Cambridge University Press)
[3] Chrzanowski H M, Walk N, Assad S M, Janousek J, Hosseini S, Ralph T C, Symul T and Lam P K 2014 *Nat. Photon.* **8** 333
Brask J B, Rigas I, Polzik E S, Andersen U L and Sørensen A S 2010 *Phys. Rev. Lett.* **105** 160501
[4] Jeong H and Kim M S 2002 *Phys. Rev.* A **65** 042305
[5] Myers C R and Ralph T C 2011 *New J. Phys.* **13** 115015
Ralph T C, Gilchrist A, Milburn G J, Munro W J and Glancy S 2003 *Phys. Rev.* A **68** 042319
[6] Lund A P, Ralph T C and Haselgrove H L 2008 *Phys. Rev. Lett.* **100** 030503
[7] Neergaard-Nielsen J S, Eto Y, Lee C-W, Jeong H and Sasaki M 2013 *Nat. Photon.* **7** 439
Furusawa A, Sörensen J L, Braunstein S L, Fuchs C A, Kimble H J and Polzik E S 1998 *Science* **282** 706
Candia Di R, Fedorov K G, Zhong L, Felicetti S, Menzel E P, Sanz M, Deppe F, Marx A, Gross R and Solano E 2015 *EPJ Quantum Technol.* **2** 25
[8] Sanders B C 2012 *J. Phys. A: Math. Theor.* **45** 244002
Sanders B C 1992 *Phys. Rev.* A **45** 6811 and references therein
[9] Joo J, Munro W J and Spiller T P 2011 *Phys. Rev. Lett.* **107** 083601
[10] Laghaout A, Neergaard-Nielsen J S, Rigas I, Kragh C, Tipsmark A and Andersen U L 2013 *Phys. Rev.* A **87** 043826
[11] Jeong H, Lund A P and Ralph T C 2005 *Phys. Rev.* A **72** 013801
Lund A P, Jeong H, Ralph T C and Kim M S 2004 *Phys. Rev.* A **70** 020101(R)
Etesse J, Bouillard M, Kanseri B and Tualle-Brouri R 2015 *Phys. Rev. Lett.* **114** 193602

[12] Ourjoumtsev A, Tualle-Brouri R, Laurat J and Grangier P 2006 *Science* **312** 83
Ourjoumtsev A, Jeong H, Tualle-Brouri R and Grangier P 2007 *Nature* **448** 784
Govia L C G, Pritchett E J and Wilhelm F K 2014 *New J. Phys.* **16** 045011
Neergaard-Nielsen J S, Nielsen B M, Hettich C, Mølmer K and Polzik E S 2006 *Phys. Rev. Lett.* **97** 083604 and references therein
[13] Clerk A A, Devoret M H, Girvin S M, Marquardt F and Schoelkopf R J 2010 *Rev. Mod. Phys.* **82** 1155
[14] Parigi V, Zavatta A, Kim M and Bellini M 2007 *Science* **317** 1890 and references therein
[15] Zavatta A, Fiurášek J and Bellini M 2014 *Nat. Photon.* **8** 564
McMahon N A, Lund A P and Ralph T C 2014 *Phys. Rev.* A **89** 023846
Xiang G Y, Ralph T C, Lund A P, Walk N and Pryde G J 2010 *Nat. Photon.* **4** 316
Donaldson R J, Collins R J, Eleftheriadou E, Barnett S M, Jeffers J and Buller G S 2015 *Phys. Rev. Lett.* **114** 120505
[16] Ferreyrol F, Barbieri M, Blandino R, Fossier S, Tualle-Brouri R and Grangier P 2010 *Phys. Rev. Lett.* **104** 123603
Ferreyrol F, Blandino R, Barbieri M, Tualle-Brouri R and Grangier P 2011 *Phys. Rev.* A **83** 063801
Pandey S, Jiang Z, Combes J and Caves C M 2013 *Phys. Rev.* A **88** 033852
Jeffers J 2011 *Phys. Rev.* A **83** 053818
Jeffers J 2010 *Phys. Rev.* A **82** 063828
Eleftheriadou E, Barnett S M and Jeffers J 2013 *Phys. Rev. Lett.* **111** 213601
Fiurášek J 2009 *Phys. Rev.* A **80** 053822
Pegg D T, Phillips L S and Barnett S M 1998 *Phys. Rev. Lett.* **81** 1604
[17] Jeong H, Zavatta A, Kang M, Lee S-W, Costanzo L S, Grandi S, Ralph T C and Bellini M 2014 *Nat. Photon.* **8** 564
Park J, Joo J, Zavatta A, Bellini M and Jeong H 2016 *Optics Express* **24** 1331
[18] Leghtas Z *et al* 2015 *Science* **347** 853
Roy A, Leghtas Z, Stone A D, Devoret M H and Mirrahimi M 2015 *Phys. Rev.* A **91** 013810
[19] Vlastakis B, Kirchmair G, Leghtas Z, Nigg S E, Frunzio L, Girvin S M, Mirrahimi M, Devoret M H and Schoelkopf R J 2013 *Science* **342** 607
[20] Hofheinz M *et al* 2009 *Nature* **459** 546
[21] Everitt M J, Spiller T P, Milburn G J, Wilson R D and Zagoskin A M 2014 *Frontiers ICT* **1** 1
Gilles L and Knight P L 1993 *Phys. Rev.* A **48** 1582
[22] Leghtas Z, Kirchmair G, Vlastakis B, Schoelkopf R J, Devoret M H and Mirrahimi M 2013 *Phys. Rev. Lett.* **111** 120501
[23] Mirrahimi M, Leghtas Z, Albert V V, Touzard S, Schoelkopf R J, Jiang L and Devoret M H 2014 *New J. Phys.* **16** 045014
[24] Bishop L S, Chow J M, Koch J, Houck A A, Devoret M H, Thuneberg E, Girvin S M and Schoelkopf R J 2009 *Nat. Phys.* **5** 105
Bishop L S 2010 *PhD Thesis* Yale University (arXiv:1007.3520)
[25] Potocek V, Miatto F M, Mirhosseini M, Magaña-Loaiza O S, Liapis A C, Oi D K L, Boyd R W and Jeffers J 2015 *Phys. Rev. Lett.* **115** 160505 ($\hat{E}^{\dagger}$ is an isomorphism but is not unitary since $\hat{E}^{\dagger}\hat{E} \neq \mathbb{I}$)
[26] Kuhn A, Hennrich M, Bondo T and Rempe G 1999 *Appl. Phys.* B **69** 373
[27] Parkins A S, Marte P, Zoller P and Kimble H J 1993 *Phys. Rev. Lett.* **71** 3095
Parkins A S, Marte P, Zoller P, Carnal O and Kimble H J 1995 *Phys. Rev.* A **51** 1578
[28] Zou X, Shu J and Guo G 2006 *Phys. Lett.* A **359** 117
[29] Oi D K L, Potoček V and Jeffers J 2013 *Phys. Rev. Lett.* **110** 210504
[30] Johnson B R *et al* 2010 *Nat. Phys.* **6** 663
[31] Ginossar E, Bishop L S, Schuster D I and Girvin S M 2010 *Phys. Rev.* A **82** 022335
[32] Heeres R W, Vlastakis B, Holland E, Krastanov S, Albert V V, Frunzio L, Jiang L and Schoelkopf R J 2015 *Phys. Rev. Lett.* **115** 137002
[33] Johnson B R 2011 *PhD Thesis* Yale University
[34] Falci G, Cognata A, La, Berritta M, D'Arrigo A, Paladino E and Spagnolo B 2013 *Phys. Rev.* B **87** 214515
[35] Masluk N A 2012 *PhD Thesis* Yale University
[36] Leek P J, Filipp S, Maurer P, Baur M, Bianchetti R, Fink J M, Göppl M, Steffen L and Wallraff A 2009 *Phys. Rev.* B **79** 180511(R)
Wallraff A, Schuster D I, Blais A, Gambetta J M, Schreier J, Frunzio L, Devoret M H, Girvin S M and Schoelkopf R J 2007 *Phys. Rev. Lett.* **99** 050501
[37] Alsing P, Guo D S and Carmichael H J 1992 *Phys. Rev.* A **45** 5135
[38] Blais A, Huang R S, Wallraff A, Girvin S M and Schoelkopf R J 2004 *Phys. Rev.* A **69** 062320
[39] Johansson J R, Nation P D and Nori F 2013 *Comp. Phys. Comm.* **183** 1760
[40] Amniat-Talab M, Lagrange S, Guérin S and Jauslin H R 2004 *Phys. Rev.* A **70** 013807
[41] Devoret M H and Schoelkopf R J 2013 *Science* **339** 1169
[42] Sun L *et al* 2014 *Nature* **511** 444
[43] Reagor M *et al* 2015 arXiv:1508.05882
[44] Sharma R and Strauch F W 2015 arXiv:1503.02157
[45] Um M, Zhang J, Lv D, Lu Y, An S, Zhang J-N, Nha H, Kim M S and Kim K 2015 arXiv:1506.07268.
[46] Manucharyan V E, Koch J, Glazman L I and Devoret M H 2009 *Science* **326** 113
Zhu G and Koch J 2013 *Phys. Rev.* B **87** 144518
[47] Král P, Thanopulos I and Shapiro M 2007 *Rev. Mod. Phys.* **79** 53
Møller D, Sørensen J L, Thomsen J B and Drewsen M 2007 *Phys. Rev.* A **76** 062321
[48] Dresea K and Holthausb M 1999 *Eur. Phys. J.* D **5** 119
Unanyan R, Guérin S, Shore B W and Bergmann K 2000 *Eur. Phys. J.* D **8** 443
[49] Malinovsky V S and Tannor D J 1997 *Phys. Rev.* A **56** 4929
Vitanov N V, Shore B W and Bergmann K 1998 *Eur. Phys. J.* D **4** 15